



Synthesis of Chalcone and Hydroxyapatite Incorporated Polyvinyl Pyrrolidone Composite Nanofibers via Electrospinning for Biomedical Application

Savari Susila G¹, P. Wilson²

¹ Department of Chemistry, St. Joseph's College (Autonomous), Tiruchirappalli-620 002, Tamilnadu, INDIA, E-mail: susilamary20@gmail.com

² Department of Chemistry, Madras Christian College (Autonomous), Chennai-600 059, Tamilnadu, INDIA

Abstract: Electrospinning is a powerful processing technique with huge potential in many attractive research fields. This technique allows nanofibrous materials including polymers and metals with a wide range of morphologies and functionalities. In the present work, an effect has been made successfully to blend the Chalcone with a biocompatible polymer and hydroxyapatite so as to make electrospun fiber nanocomposite. This report is the first of its kind with regard to the chalcone, polyvinyl pyrrolidone and hydroxyapatite combination. The product fiber nanocomposite was characterized by XRD, FTIR, FESEM.EDAX and Antibacterial activities. The obtained composite nanofibers were desirable products to be utilized as excellent antibacterial filters and as wound healing agents.

KEYWORDS: *electrospinning; fiber nanocomposite; chalcone; polyvinyl pyrrolidone; hydroxyapatite.*

I.INTRODUCTION

Electrospinning is a versatile and efficient method to produce continuous nanofibers from submicron diameters down to nanometer diameters by using a high potential electric field. It is possible to produce nanofibers with diameters ranging from a few nanometers to a few hundred nanometers thanks to the latest developments in electrospinning [1, 2]. The technique can easily be employed in the laboratory and can be scaled up to an industrial process [3]. Electrospinning of nanofibers from polymer solutions or melts has been a focus of interest as they have many potential applications [4]. The electro-spun fibers are mostly deposited on electrode collectors in the form of a nonwoven nanofiber mat. It is also possible to obtain aligned nanofibers by using controlled fiber deposition techniques [5].

Electrospinning is applicable to a wide range of materials such as synthetic and natural polymers, metals as well as ceramics, and composite systems [6]. It consists of layered nanofiber nonwoven material. Electrospun nanofiber mats offer considerable increases in filtering capability [7]. The electrospinning method

is very suitable to process natural polymers and synthetic biocompatible or bioabsorbable polymers for biomedical applications [8]. Conductive polymers are interesting in this respect. Insulating polymers were also used, but ions or nanofillers were added to improve conductivity [9].

Polymeric conductive membranes are also considered to have potential use in electromagnetic interference shielding, photovoltaic devices, electrostatic dissipation, production of tiny electronic devices, sensors, actuators, etc [10]. Various types of polymers have been combined with calcium phosphates (mainly hydroxyapatite) to prepare nanocomposites with improved biocompatible and mechanical properties [11,12]. PVP is available in different grades based on molecular weights. It is mainly used as a binder in tablet formulations. When compared to other binders, wet granulation with PVP having a molecular weight of 25,000 to 90,000 generally gives harder granulates with good flow ability, higher binding, and low friability [13,14]. Chalcones are used to synthesize several derivatives like cyanopyridines, pyrazolines isoxazoles, and pyrimidines having different heterocyclic ring systems [15-17]. Synthetic derivatives (i.e chalcone here) are often found to be more active than parent compounds [18-20].

The present investigation is aimed at synthesizing nanocomposite fibers by electrospinning method, to characterize the same for its structure and morphological features.

The objective of the present investigation is

- i) To synthesize a chalcone namely
 - (2E)-1(4-hydroxyphenyl)-3(4-hydroxy-3-ethoxy phenyl)-2-propen-1-one by acid-catalyzed Claisen-Schmidt reaction in absolute alcohol
- ii) To prepare hydroxyapatite [HAP-1] using the ultrasonication method
- iii) To prepare hydroxyapatite [HAP-2] using the hydrothermal method
- iv) To generate three electrospun nanofiber composites namely
 - Dihydroxychalcone-polyvinyl pyrrolidone composite
 - Dihydroxychalcone-polyvinyl pyrrolidone-HAP-1 composite and
 - Dihydroxychalcone-polyvinyl pyrrolidone-HAP-2 composite
- v) To characterize the three electrospun nanofibers using appropriate analytical techniques like FT-IR, powder XRD and FESEM techniques
- vi) To establish their bactericidal activity using the Disc diffusion method

II.METHODOLOGY

The chapter explains the detailed information about chemicals used for the experimental part related to the synthesis of chalcone, hydroxyapatite and nanocomposite fibers. In addition, instruments used to characterize the phase transition, morphology of nanofibers have been reported in detail.

2.1 Materials

All the chemicals and reagents used in this research work were in AR grade. The following chemicals are used in this research work:

- 4-hydroxy acetophenone (SD Fine-Chem. Ltd.),
- 4-hydroxy-3-ethoxybenzaldehyde (SD Fine-Chem. Ltd.),
- Absolute alcohol (SD Fine-Chem. Ltd.),
- Sodium chloride (SD Fine-Chem. Ltd.),
- Sulphuric acid (SD Fine-Chem. Ltd.),
- Calcium nitrate (SD Fine-Chem. Ltd.),
- Diammonium hydrogen Phosphate (Merck Specialties Pvt. Ltd.)
- Liquor ammonia (Qualigens fine chemicals)
- Triton X-100 (Sisco Research Laboratories Pvt. Ltd.)
- L-Arginine (Qualigens fine chemicals)
- Polyvinyl pyrrolidone (Qualigens fine chemicals)
- N, N-dimethyl formamide (DMF) (Qualigens fine chemicals)

2.2 Preparation of Chalcone

Chalcone diol was prepared by acid-catalyzed Claisen-Schmidt reaction. Dry HCl gas was passed for one hour through a well-cooled and stirred solution of 4-hydroxy acetophenone (0.05 mol) and 4-hydroxy-3-ethoxybenzaldehyde (0.05 mmol) in 120 mL of absolute alcohol in a 250 mL round-bottomed flask. A wine red-colored solution was formed. In addition to a sufficient quantity of ice-cold water, a yellow precipitate of (2*E*)-3-(4-hydroxy-3-ethoxy phenyl)-1-(4-hydroxyphenyl) prop-2-en-1-one was formed, which was filtered, then washed with double distilled water and finally allowed to dry. The dried product was recrystallized from hot ethanol. A schematic of the synthesis is given in Fig. 1.

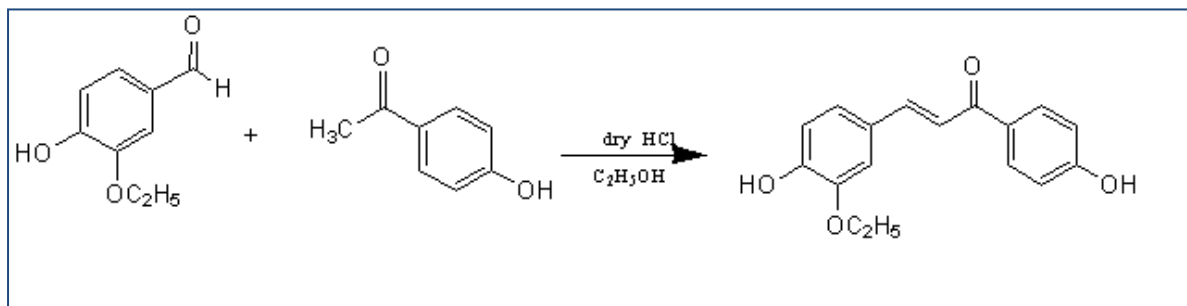


Fig. 1 Synthesis of Chalcone

2.3 PREPARATION OF HYDROXYAPATITE

2.3.1 Ultrasonication method (HAP-1)

Aqueous solutions of 0.4 M calcium nitrate tetrahydrate $\text{Ca}(\text{NO}_3)_2 \cdot 4\text{H}_2\text{O}$ and 0.2395 M $(\text{NH}_4)_2\text{PO}_4$ were prepared using deionized water. Typically, calcium/amino acid solution was prepared by dissolving an appropriate amount of the amino acid (6.968 g of L-Arginine) into a calcium solution under gentle stirring. The ratio of calcium salt and L-arginine was fixed to be 1:1. Calcium/amino acid solution was slowly added into diammonium hydrogen phosphate solution, which was also maintained at pH 10.2. The entire reaction was carried out under ultrasonication. Upon completion of the addition of reactants; the as obtained white suspension was centrifuged, washed repeatedly with deionized water, and allowed to dry at 120 °C in a hot air oven for 2 h. Then the sample was calcined at 600 °C for 2 h. the sample is labeled as HAP-1.

2.3.2 Hydrothermal method (HAP- 2)

About 100 mL of 0.24 M $(\text{NH}_4)_2\text{PO}_4$ (pH 10.4; adjusted using 1:1 NH_3) was taken in a 500 mL beaker and 100 mL of 0.4 M solution of $\text{Ca}(\text{NO}_3)_2$ (pH 10.4; adjusted using 1:1 NH_3) containing 4% Triton X-100 (w/v) was added drop-wise from a burette while stirring the content of the beaker using a magnetic stirrer. Adequate care was taken to maintain the pH of the reaction mixture above 10. A milky suspension was formed and refluxed for an hour, cooled and centrifuged. The white precipitate thus obtained was dried overnight in a hot air oven at 120 °C and a portion of it was calcined at 600 °C for 2 h in air ambiance. The sample is designated as HAP-2 .

2.4 ELECTROSPINNING PROCESS

2.4.1 Precursor preparation for electrospinning

a) Precursor for Nanofiber Composite-1

Polyvinyl pyrrolidone (0.4 g) was dissolved in 5 ml of DMF solvent and taken in a round bottom flask. It was stirred for 1-2 h. To this (0.1 g) of chalcone was added slowly with continuous stirring for 10 min. The mixing was continued for another 2–3 h at room temperature. The final homogenous mixture was used for electrospinning.

b) Precursor for Nanofiber Composite-2

Here, the solution was prepared as explained above. However, HAP-1 was added and continuously stirred for 20 min. The final homogenous mixture was used for electrospinning.

c) Precursor for Nanofiber Composite-3

The solution prepared for electrospinning was similar to the above preparation. However, HAP-1 was replaced with HAP-2. The final homogenous mixture was used for electrospinning.

2.4.2 Electrospinning of the precursor

In all the cases, electrospinning was performed at room temperature at a voltage of 15 kV. A grounded iron drum was rotated at a constant speed by a DC motor to collect the developing nanofibers, which were kept at a distance of 15 cm from the micro-tip. Later, the developed nanofiber mats over the Al foil collector attached to the rotating drum were collected and vacuum dried for 24 h. The resultant nanofiber mats were labeled as Nanofiber Composite-1 (NFC-1), Nanofiber Composite-2 (NFC-2) and Nanofiber Composite-3 (NFC-3), and utilized for further characterization

III. RESULTS AND DISCUSSION

Three electrospun nanofibers composite NFC-1, NFC-2 and NFC-3 were characterized by FESEM, EDAX, XRD and FT-IR. The Agar Disc diffusion method was employed to establish its bactericidal activity.

3.1 Fourier Transform Infrared Spectral Studies

The structural configurations of NFC-1, NFC-2 and NFC-3 were characterized by using FT-IR spectroscopy and are shown in Fig. 8. The characteristic peaks of NFC-1 were observed at 1405 cm^{-1} (CH_2 bending vibration); 1201 cm^{-1} , 1059 cm^{-1} (C-N vibration frequency) can be ascribed to polyvinyl pyrrolidone in the composite. Some shifts were observed in the FT-IR spectra of chalcone blended PVP composite nanofibers. The transmittance bands centered at 1641 , 1649 and 1641 cm^{-1} correspond to C=O stretching frequency present in the chalcone in NFC-1.

Transmittance peaks were observed for the NFC-2 and NFC-3 around 3460 , 3378 and 3468 cm^{-1} corresponding to O-H stretching frequency present in the chalcone. The bands corresponding to 1469 , 1405 , 803 and 855 cm^{-1} implies the presence of carbonate ion in the resultant HAP's.

The broad transmittance bands at 633 and 3460 cm^{-1} correspond to $-\text{OH}$ stretching vibration. Transmittance peaks were seen for NFC-1 and NFC-2 around 1073 , 1059 , 603 , 535 and 431 cm^{-1} corresponds to PO_4^{3-} ions present in the sample. Moreover, peaks at 1093 , 1088 , 1036 and 962 cm^{-1} correspond to PO_4^{3-} stretching vibration.

These FT-IR spectra confirm the successful preparation of drug-incorporated PVP composite nanofibers.

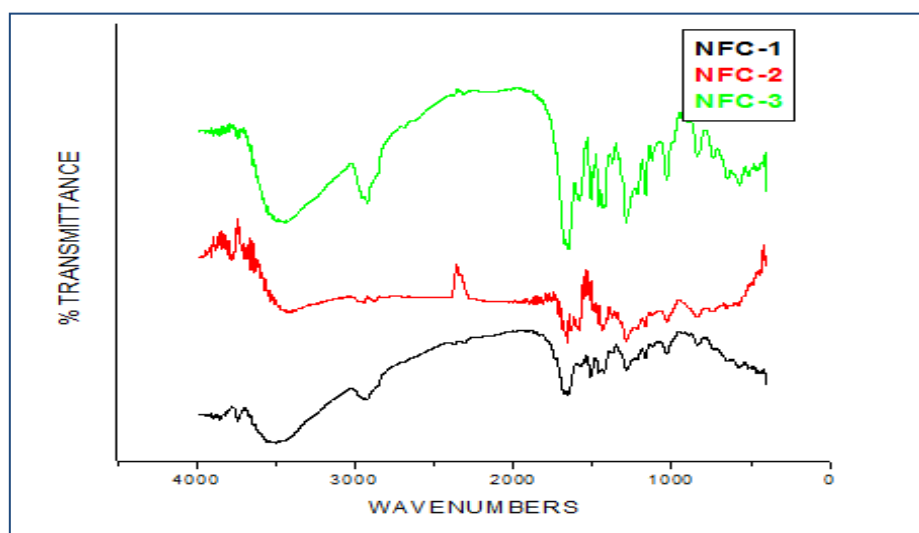


Fig. 2 FT-IR Spectra of (a) NFC-1 (b) NFC-2 (c) NFC-3

Table. 1 IR characteristic bands of PVP composite nanofibers

Assignments	IR frequency (cm⁻¹)
PO ₄ ³⁻ bending modes	1073,1059, 603, 535, 431
PO ₄ ³⁻ stretching modes	1093, 1088, 1036, 962
Carbonate	1405, 1469, 803, 855
Structural OH	3460, 633
Chalcone (C=O stretching frequency) (O-H stretching frequency)	1641,1649,1641 3460, 3378, 3468
PVP (C-N vibration frequency)	1059, 1201
PVP (CH ₂ - bending modes)	1405

3.2 X-Ray Diffraction Studies

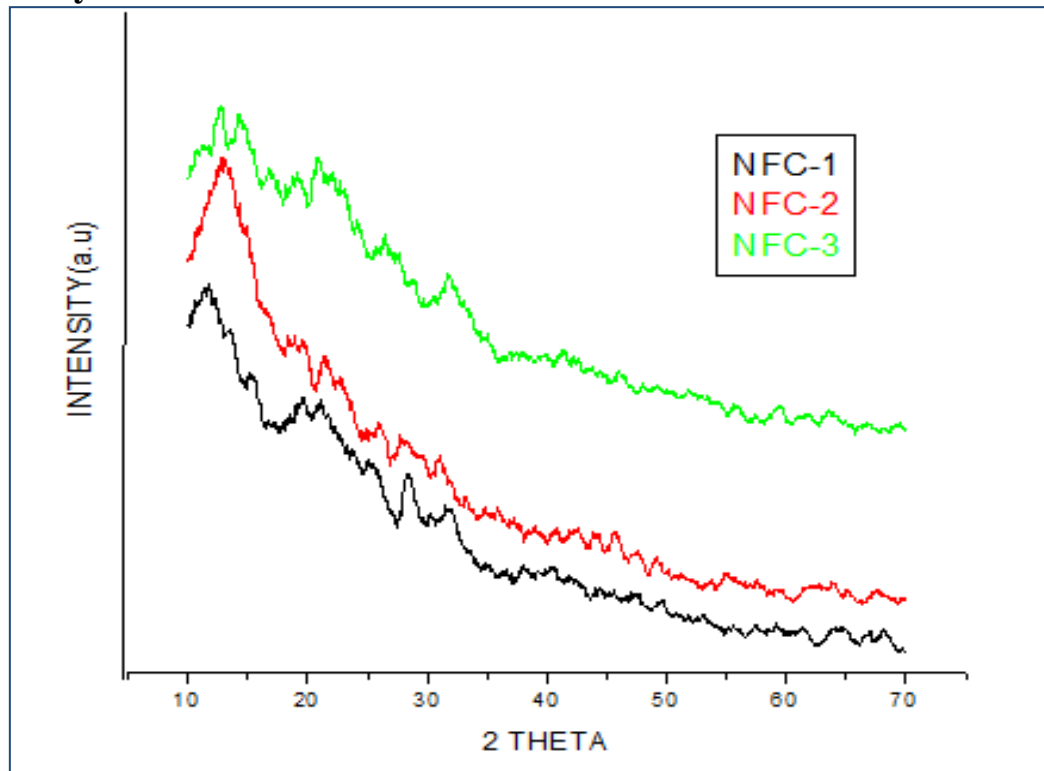


Fig. 3 XRD patterns of (a) NFC-1 (b) NFC-2 (c) NFC-3

XRD analysis was employed to investigate the phase structures of the NFC-1, NFC-2 and NFC-3. The XRD diffractograms of the composite nanofibers are shown in Fig. 3. The XRD patterns revealed that the NFC-2 and NFC-3 were partially crystalline. At the same time, the diffraction pattern corresponding to the NFC-1 appears to be slightly sharper. The presence of HAP nanoparticles in the NFC-2 and NFC-3 was confirmed by XRD diffraction peaks at 2θ values 26.0, 31.24 and 26.67, 31.86 respectively, corresponding to (002) and (211) main reflection planes of apatite-like calcium phosphate (JCPDS no. 09-0432). However, in the case of NFC-1, the incorporation of the drug did not reveal any structural changes due to the low concentration of loading. No significant diffraction peaks of any other phases or impurities can be detected in the XRD patterns, which indicate the successful formation of NFC-1, NFC-2 and NFC-3 void of impurities [21].

3.3 Field Emission Scanning Electron Microscopy

FESEM images of the as-obtained NFC-1, NFC-2 and NFC-3 were shown in Fig. 4,5 and 6. As observed in these figures, composite nanofibers were found to be smooth and flexible. However, the morphological appearance of the composite nanofiber slightly differed from each other. The diameter of the nanofibers was in the range of 100 – 200 nm. In the case of NFC-2 and NFC-3 there appear to be outwarding protruded nanofibers at the periphery with more beads formation.

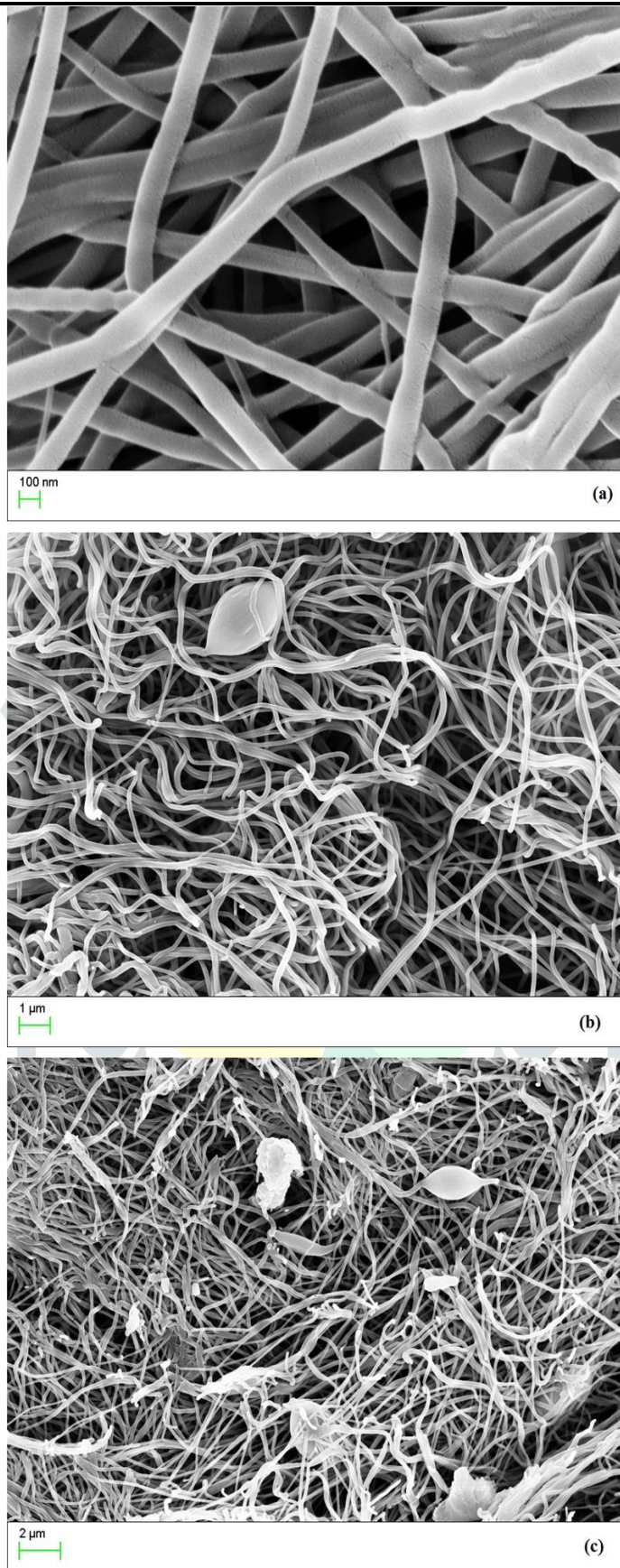


Fig. 4 FESEM images of NFC-1 a) 100 nm, b) 1 μm, c) 2 μm

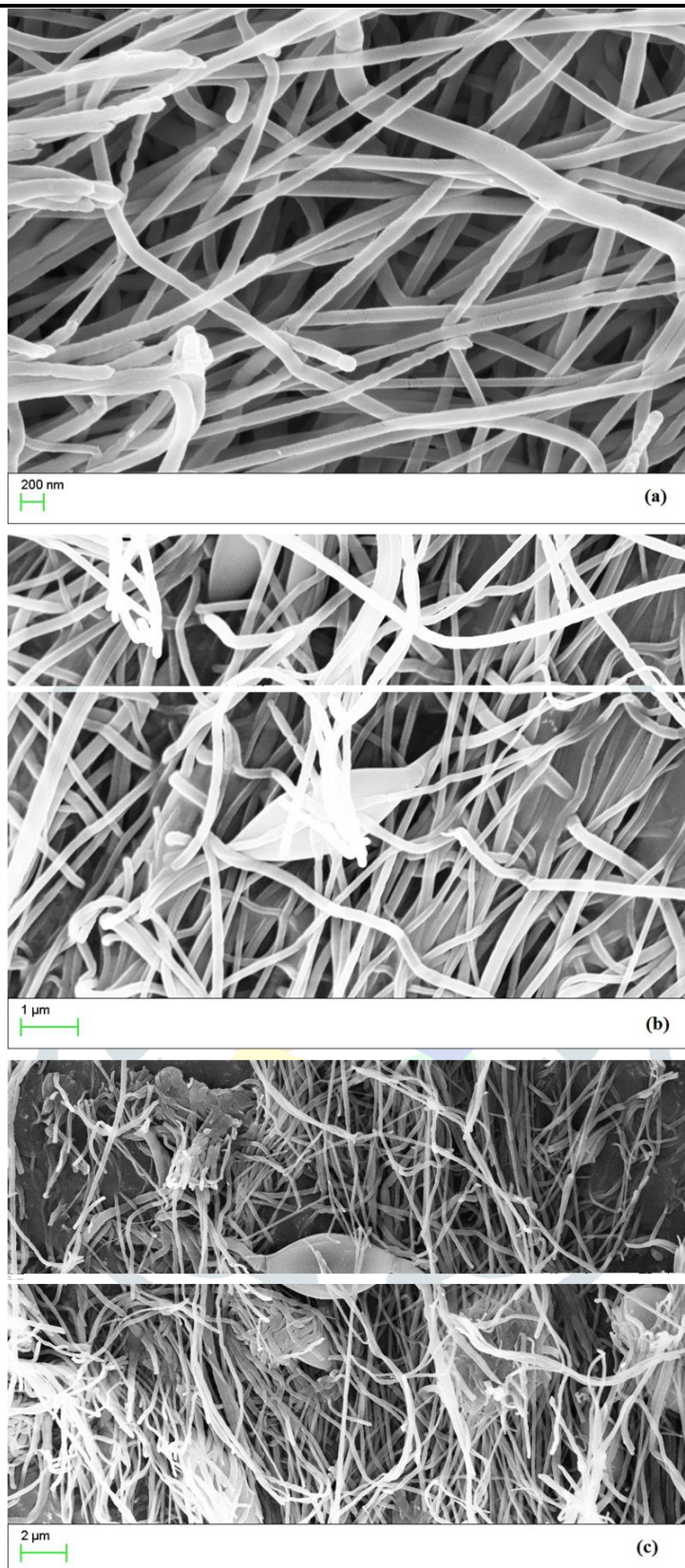


Fig. 5 FESEM images of NFC-2 a) 200 nm, b) 1 μm, c) 2 μm

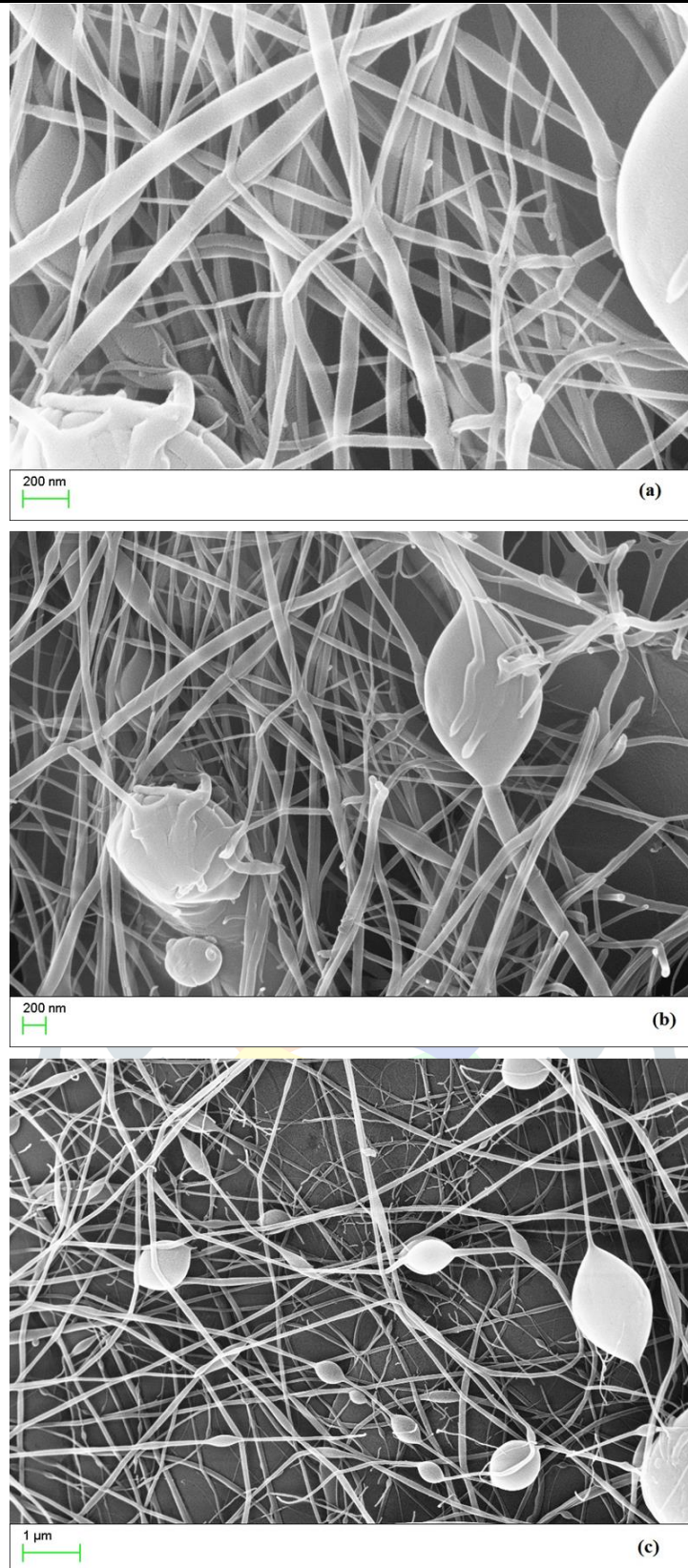


Fig. 6 FESEM images of NFC-3 a) 200 nm, b) 1 μ m, c) 2 μ m

3.4 Energy Dispersion X-Ray Analysis

The elemental composition of the as-prepared nanofibers was analyzed using EDAX attached to FESEM. NFC-1 (Fig. 7a) showed the peaks for C and O, without the presence of other impurities. However, NFC-2 (Fig. 7b) and NFC-3 (Fig. 7c) showed a large percentage of Ca and O indicating the incorporation of HAP into the nanocomposite fibers. The result correlates well with the FESEM images as the HAP incorporation has made its morphological effects in the nanocomposites.

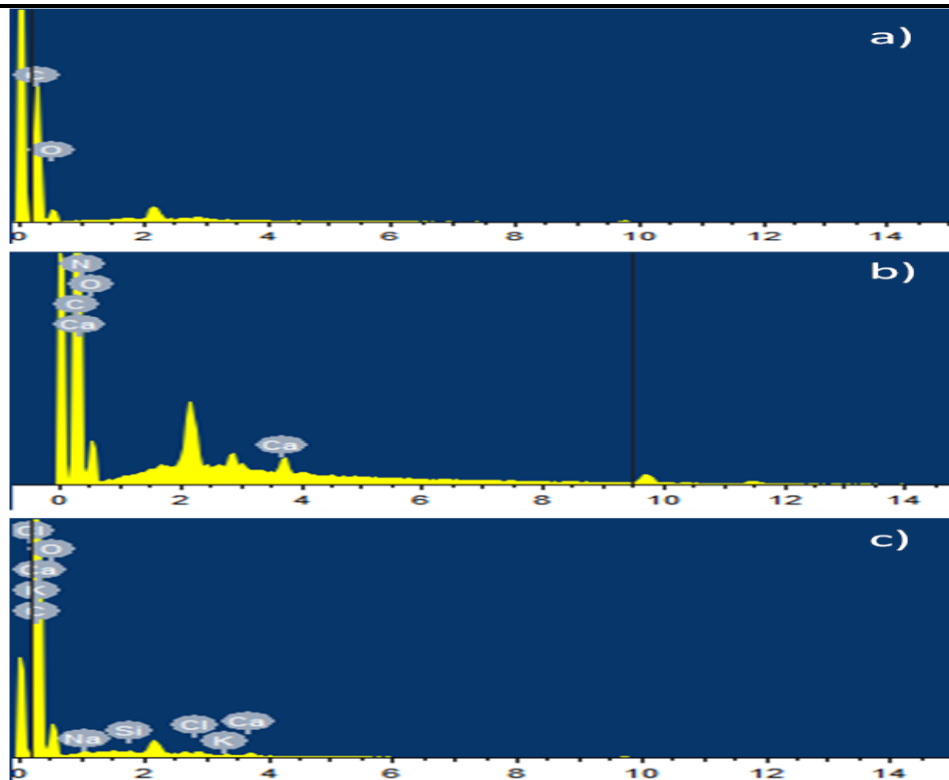


Fig. 7 EDAX of a) NCF-1 b) NCF-2 c) NCF-3

3.5 Antibacterial Studies

The disc diffusion method was employed to establish the bactericidal efficacy of the NFC-1, NFC-2 and NFC-3 against certain gram-positive (*Staphylococcus aureus* and *Bacillus subtili*) and gram-negative bacteria (*Escherichia coli* and *Klebsiella pneumoniae*) was performed on the MHA plate at an incubation temperature of 37 °C. The zone of inhibition was observed after 24 h of incubation and the diameter of the zone was measured. Fig. 8-11 shows the bactericidal activities of composite nanofibers NFC-1, NFC-2 and NFC-3.

Tables 2, 3, 4 and 5 represent the inhibition effects of the composite nanofibers on the growth of selected gram-positive and gram-negative bacteria. The pictorial representation of the inhibition effects is given in Fig. 12-15.

More pronounced bactericidal effect was observed for the NFC-1, NFC-2 and NFC-3 which are shown in Fig. 8-11. The test was repeated and the results were found to be similar. The plates were checked for a prolonged incubation time to study the efficiency of the drug release. It is a known factor that the decontamination of exogenous organisms is a critical factor as a wound-healing material. The anti-bacterial property plays a crucial role in the electrospun-based wound dressing membranes. As the interconnected nanofibers create perfect blocks and pores in the nanofiber membrane, the nanofiber membrane should be able to prevent any bacteria from penetrating, therefore avoiding exogenous infections effectively. The results showed that our composite mat is a good antibacterial membrane and it can be applied as a perfect wound dressing material.

The results show that all the as-prepared samples NFC-2 and NFC-3 possess strong bactericidal activity better than NFC-1 for both Gram-positive (*Staphylococcus aureus* and *Bacillus subtilis*) and Gram-negative (*Escherichia coli* and *Klebsiella pneumoniae*) bacteria.

This is because there were plenty of drug particles that can be readily available on the periphery of the NFC-2 and NFC-3 samples. Thus, we can conclude that the obtained composite nanofibers were desirable candidates to be utilized as excellent antibacterial filters and also as wound healing agents.

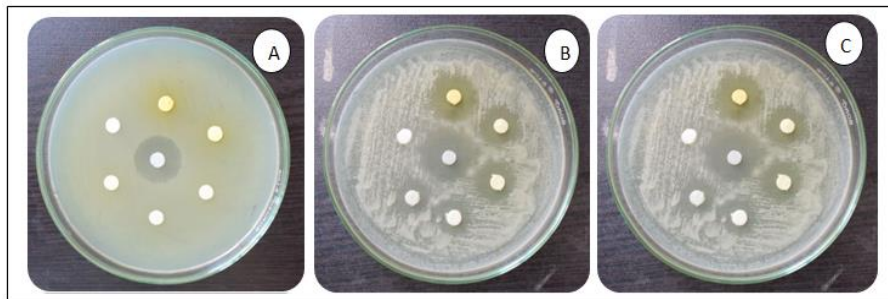


Fig.8 Bactericidal activity of *Staphylococcus aureus* exposed to (a) NFC-1 (b) NFC-2(c) NFC-3

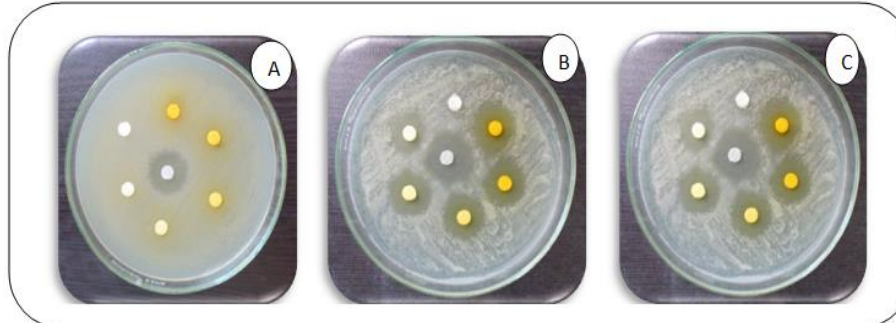


Fig.9 Bactericidal activity of *Bacillus subtilis* exposed to (a) NFC-1 (b) NFC-2 (c) NFC-3

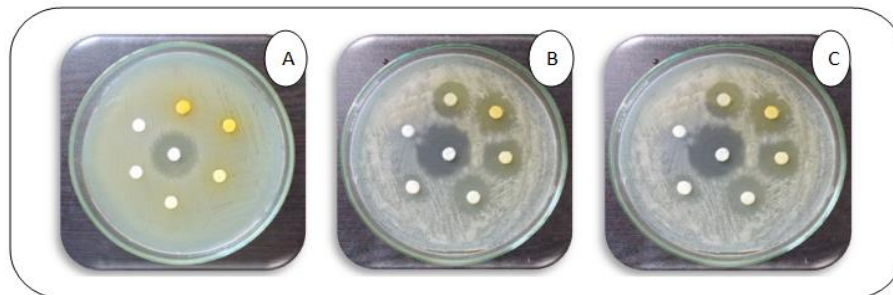


Fig.10 Bactericidal activity of *Escherichia coli* exposed (a) NFC-1(b) NFC-2 (c) NFC-3

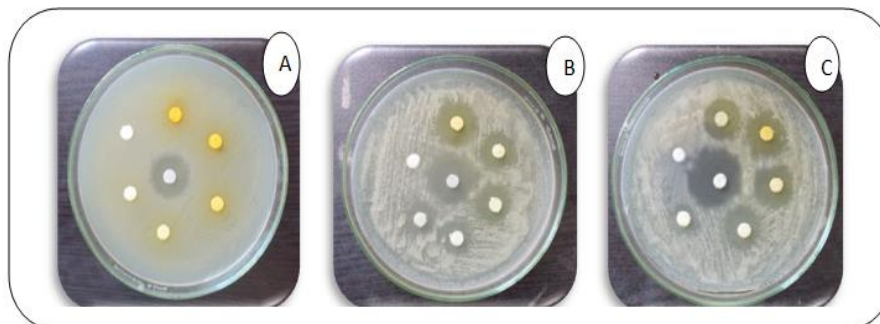


Fig.11 Bactericidal activity of *Klebsilla pneumoniae* exposed to (a) NFC-1 (b) NFC-2 (c) NFC-3

Table 2 Inhibition effects of the three composite nanofibers on the growth of *Staphylococcus aureus*

Nanofiber Composite	Zone of Inhibition in mm of <i>Staphylococcus aureus</i>					
	500 µg	250 µg	125 µg	62.5µg	31.2µg	DMSO
NFC-1	7	6	6	4	4	6
NFC-2	9	8	8	7	5	6
NFC-3	9	8	8	6	6	6

Table 3 Inhibition effects of the three composite nanofibers on the growth of *Bacillus subtilis*

Nanofiber Composite	Zone of Inhibition in mm of <i>Bacillus subtilis</i>					
	500 µg	250 µg	125 µg	62.5µg	31.2µg	DMSO
NFC-1	8	7	6	4	4	6
NFC-2	10	9	8	6	7	6
NFC-3	10	9	7	6	5	6

Table 4 Inhibition effects of the three composite nanofibers on the growth of *Escherichia coli*

Nanofiber Composite	Zone of Inhibition in mm of <i>Escherichia coli</i>					
	500 µg	250 µg	125 µg	62.5µg	31.2µg	DMSO
NFC-1	9	8	7	5	4	6
NFC-2	10	9	8	6	7	6
NFC-3	10	9	7	6	5	6

Table 5 Inhibition effects of the three composite nanofibers on the growth of *Klebsilla pneumoniae*

Nanofiber Composite	Zone of Inhibition in mm of <i>Klebsilla pneumoniae</i>					
	500 µg	250 µg	125 µg	62.5µg	31.2µg	DMSO
NFC-1	5	4	4	3	3	5
NFC-2	7	6	6	5	4	5
NFC-3	7	6	5	5	3	5

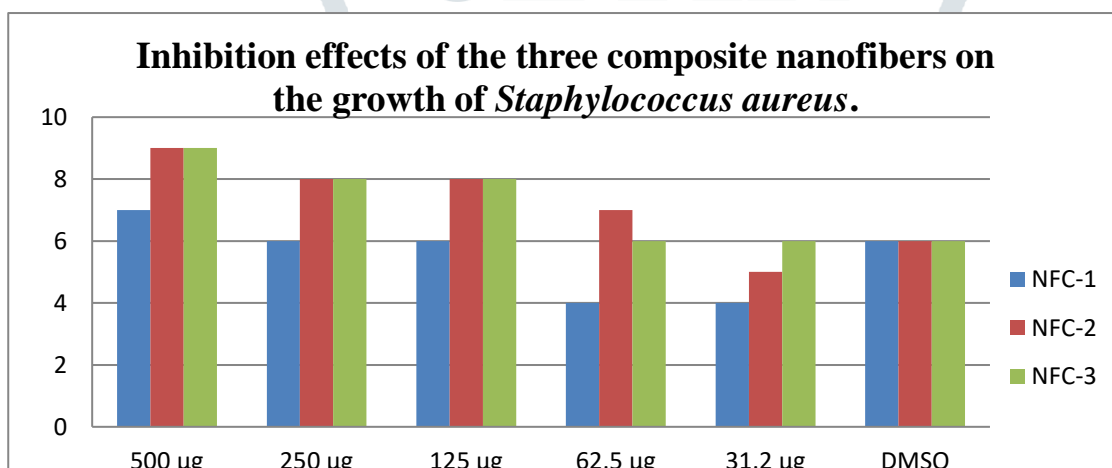


Fig.12 Inhibition effects of the three composite nanofibers on the growth of *Staphylococcus aureus*

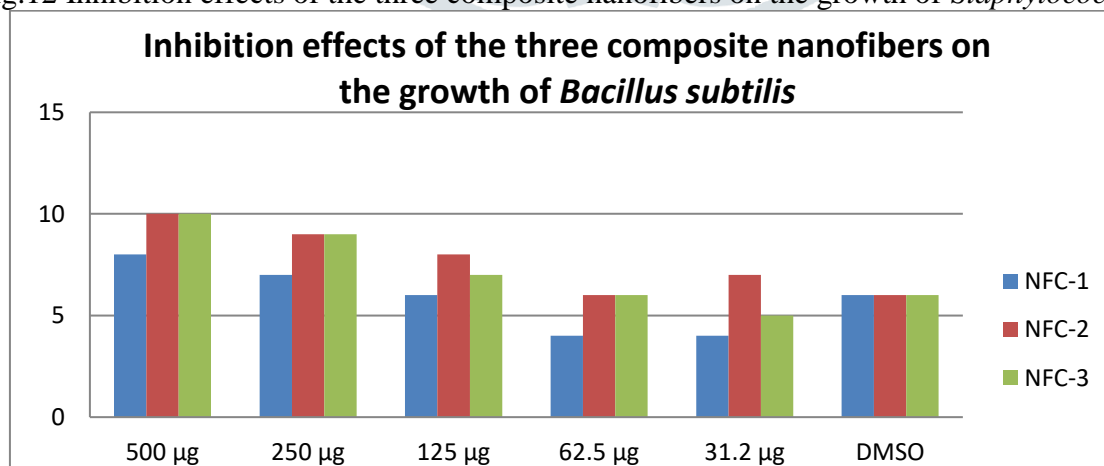


Fig.13 Inhibition effects of the three composite nanofibers on the growth of *Bacillus subtilis*

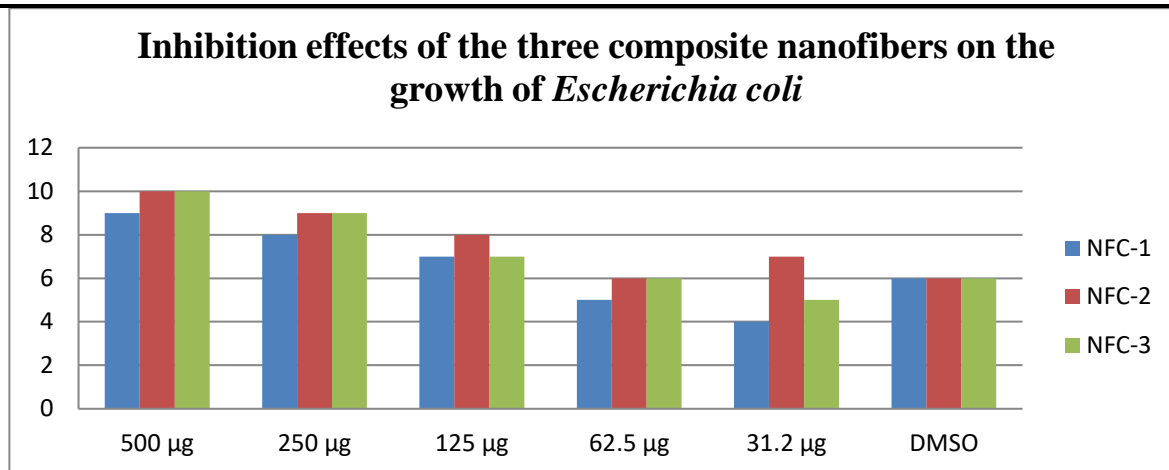


Fig.14 Inhibition effects of the three composite nanofibers on the growth of *Escherichia coli*

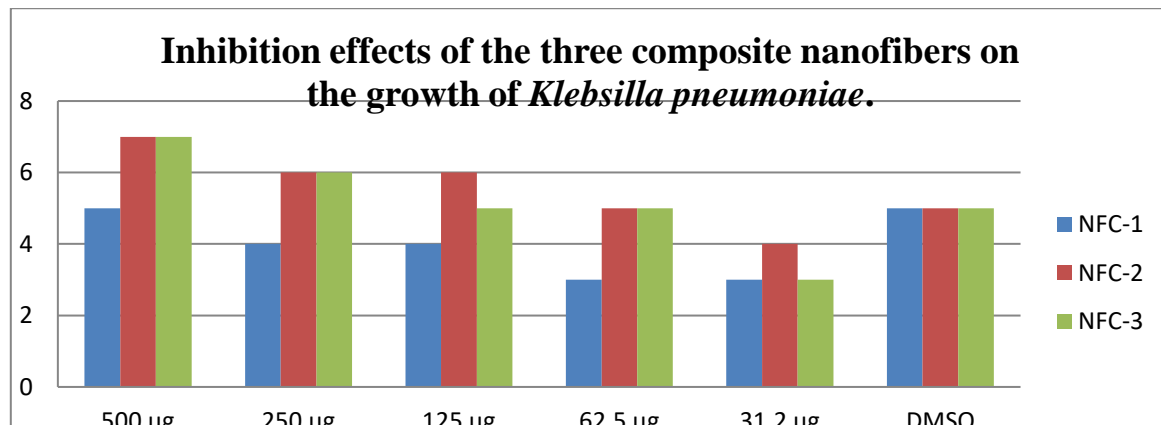


Fig.15 Inhibition effects of the three composite nanofibers on the growth of *Klebsilla pneumoniae*

IV.SUMMARY AND CONCLUSION

In the present investigation, an effort has been made successfully to blend the chalcone with a biocompatible polymer and hydroxyapatite so as to make the electrospun fiber nanocomposite. To the best of our knowledge, this report is the first of its kind with regard to the chalcone, polyvinyl pyrrolidone and hydroxyapatite combination.

The XRD data clearly confirmed the presence of apatite-like materials in NFC-2 and NFC-3. The FT-IR analysis of the samples confirms the presence of chalcone, polyvinyl pyrrolidone and calcium phosphates. FESEM images unveiled the surface morphology of the composite nanofibers formed. The elemental composition of the composite nanofibers was revealed by the EDAX analysis.

The antibacterial activity of the three composite materials screened using the Agar disc diffusion method proved them as significant antibacterial agents. Among all the three samples, chalcone-loaded hydroxyapatite samples displayed excellent antibacterial properties towards Gram-positive (*Staphylococcus aureus* and *Bacillus subtilis*) and Gram-negative (*Escherichia coli* and *Klebsiella pneumoniae*) bacterial strains than the chalcone sample. Chalcone loaded on both the hydroxyapatite showed comparable antibacterial activities in the present investigation. It is further noted that the presence of hydroxyapatite has augmented the antibacterial activity apart from serving as a biomaterial. Efforts are on to further optimize the preparation conditions so as to avoid the formation of beads during the electrospinning process.

REFERENCES

1. Venugopal, J. & Ramakrishna, S.: Applications of polymer nanofibers in biomedicine and biotechnology, *Applied Biochemistry and Biotechnology*, 125 (2005), pp. 147-157, ISSN 0273-2289

2. Ji, W.; Sun, Y.; Yang, F.; Van den Becken, J.J.J.P.; Fan, M.; Chen, Z. & Jansen, J.A.: Bioactive electrospun scaffolds delivering growth factors and genes for tissue engineering applications, *Pharmaceutical Research*, 28 (2011), pp. 1259-1272, ISSN 0724-8741
3. Liu, Y.; He, J.H.; Yu, J.Y. & Zeng, H.M.: Controlling numbers and sizes of beads in electrospun nanofibers, *Polymer International*, 57 (2008), pp. 632-636, ISSN 0959-8103
4. Bhardwaj, N. & Kundu, S.C.: Electrospinning: A fascinating fiber fabrication technique, *Biotechnology Advances*, 28 (2010), pp.325-347, ISSN 0734-9750
5. Li, D.; Wang, Y. & Xia, Y.: Electrospinning nanofibers as uniaxially aligned arrays and layer-by-layer stacked films, *Advanced Materials*, 16 (2004), 4, pp. 361-366, ISSN 1521 4095
6. Li, S.; Hashi, C.; Huang, N.F. & Kurpinski, K., Biomimetic Scaffolds, US patent, WO07090102A2, (2007)
7. Fang, J.; Wang, X. & Lin, T.: Functional applications of electrospun nanofibers - production, properties, and functional applications, Dr. Tong Lin (Ed.), Intech, ISBN: 978-953-307-420-7, (2011)
8. Venugopal, J. & Ramakrishna, S.: Applications of polymer nanofibers in biomedicine and biotechnology, *Applied Biochemistry and Biotechnology*, 125 (2005), pp. 147-157, ISSN 0273-2289
9. Fang, J.; Wang, X. & Lin, T.: Functional applications of electrospun nanofibers - production, properties, and functional applications, Dr. Tong Lin (Ed.), Intech, ISBN: 978-953-307-420-7, (2011)
10. Bhardwaj, N. & Kundu, S.C.: Electrospinning: A fascinating fiber fabrication technique, *Biotechnology Advances*, 28 (2010), pp.325-347, ISSN 0734-9750
11. Mourino V, Boccaccini AR. Bone tissue engineering therapeutics: controlled drug delivery in three-dimensional scaffolds. *J R Soc Interface*. 2010; 7:209–27. doi:10.1098/rsif.2009.0379
12. Porter JR, Ruckh TT, Popat KC. Bone tissue engineering: a review in bone biomimetics and drug delivery strategies. *Biotechnol Prog*. 2009; 25:1539–60. doi:10.1002/btpr.246
13. Chowhan, Z.T. Role of Binders in Moisture-Induced Hardness Increase in Compressed Tablets and Its Effect on *in vitro* Disintegration and Dissolution. *J. Pharm. Sci.* 1980, 69 1-4
14. Chowhan, Z.T.; Amaro, A.A.; Ong, J.T.H. Punch Geometry and Formulation Considerations in Reducing Tablet Friability and Their Effect on *in vitro* Dissolution. *J. Pharm. Sci.* 1992, 81,290-294. *Polymers* 2011, 3, 1997
15. M. A. El.Hashanah; M. El-Kady; M. A. Saiyed and A. A. Elaswy, The chemistry of heterocyclic compounds: Oxazoles, Egypt. *J.Chem.*, 27, 715 (1985)
16. L. S. Crawley and W. J. Fanshawe, The chemistry of heterocyclic compounds: Isooxazoles, *J. Heterocyclic Chem.*, 14, 531 (1977)
17. E. C. Taylor and R. W. Morrison, An unusual molecular rearrangement of an N-aminopyrimidine, *J. Org. Chem.*, 32, 2379 (1967)
18. Sirion, U.; Kasemsook, S.; Suksen, K.; Piyachaturawat, P.; Suksamrarn, A.; Saeed, R. New substituted C-19-andrographolide analogs with potent cytotoxic activities. *Bioorg. Med. Chem. Lett.* 2011, 22, 49–52

19. Lin, C.M.; Jiang, Y.Q.; Chaudhary, A.G.; Rimoldi, J.M.; Kingston, D.G.I.; Hamel, E. A convenient tubulin-based quantitative assay for paclitaxel (Taxol) derivatives is more effective in inducing assembly than the parent compound. *Cancer Chemother. Pharmacol.* 1996, 38, 136–140
20. Anand, P.; Kunnumakkara, A.B.; Newman, R.A.; Aggarwal, B.B. Bioavailability of curcumin: problems and promises. *Mol. Pharm.* 2007, 4, 807–818
21. Yuri Choi R. Nirmla, Jun Yeoub Lee, Mashiar Rahma, Seong-Tshool Hong, Hak Yong Kim Antibacterial ciprofloxacin HCl incorporated polyurethane composite nanofibers via electrospinning for biomedical applications *Ceramics International* 39 (2013) 4937–4944

